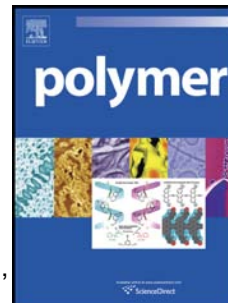# Accepted Manuscript

Polycyanurate Networks from Dehydroanethole Cyclotrimers: Synthesis and Characterization

Matthew C. Davis, Andrew J. Guenthner, Christopher M. Sahagun, Kevin R. Lamison, Josiah T. Reams, Joseph M. Mabry

Please cite this article as: Davis MC, Guenthner AJ, Sahagun CM, Lamison KR, Reams JT, Mabry JM, Polycyanurate Networks from Dehydroanethole Cyclotrimers: Synthesis and Characterization, *Polymer* (2013), doi: 10.1016/j.polymer.2013.10.050.

Star anise

Trianethole tricyanate

heat

Biobased Polycyanurate networks

Polycyanurate Networks from Dehydroanethole Cyclotrimers:

Synthesis and Characterization

Matthew C. Davis,[a,*] Andrew J. Guenthner,[b,*] Christopher M. Sahagun,[c] Kevin R. Lamison,[d]

Josiah T. Reams,[d] and Joseph M. Mabry[b]

[a]*Chemistry & Materials Division, Michelson Laboratory, Naval Air Warfare Center, China Lake, California, 93555, USA*

[b]*Air Force Research Laboratory, Aerospace Systems Directorate Edwards AFB, California, 93524, USA*

[c] *National Research Council / Air Force Research Laboratory, Aerospace Systems Directorate, Edwards AFB, California, 93524, USA*

[d]*ERC Incorporated, Edwards AFB, California, 93524,USA*

Abstract

Novel biobased trisphenols were obtained by palladium- and cobalt-catalyzed [2+2+2] cycloaddition of dehydroanethole isomers which were readily prepared from the natural product *trans*-anethole. The trisphenols were transformed into their corresponding tricyanate esters and thermally cured to give polycyanurate networks. Comparison of the thermal properties, from differential scanning calorimetry, thermogravimetric and oscillatory thermomechanical analyses, of the new tricyanate esters with similar commercial products is presented. A new tricyanate ester with an acceptable processing temperature that yields a polycyanurate with very high glass transition temperature and low water absorption was found. Interestingly, the low moisture absorption was found to help limit the degradation of residual cyanate ester groups during

* *Corresponding authors.* Tel.: 01 7609390196; *E-mail address:* matthew.davis@navy.mil (M.C. Davis); Tel.: 01 6612758020; *E-mail address:* andrew.guenthner@us.af.mil (A.J. Guenthner).

exposure to hot water, allowing for a substantial recovery in the glass transition temperature upon subsequent heating, an unusual phenomenon for polycyanurate networks.

Keywords: high temperature materials, networks, cyanate ester, polycyanurate, renewable resources, thermosets, thermal properties, cycloaddition, alkynes

1. Introduction

The enormous variety and quantity of plastics that make up the consumer goods on the market today are almost entirely composed of petrochemicals or chemicals derived from fossil based sources. Predictions are continually changing about when this invaluable natural resource, crude oil, will expire [1-4]. Of course, there is already inherent competition for the use of crude oil as a chemical feedstock [5], because of the need for liquid transportation fuels. In addition, it is clear that there will be increasing demands on this resource as economic growth and industrialization in the developing regions of the world continues at a dramatic pace [6,7]. The theoretically best solution to achieve a secure supply of chemical feedstock without the need for crude oil would be to obtain chemical building blocks from biomass [8-13]. Although this concept can present new complications and concerns, both economic and environmental in nature (e. g., arable land, water, fertilizer, climate, etc.), these concerns are far beyond the scope of the present theme. Rather, we focus on the fact that, as Dijkstra and Langstein [14] recently pointed out, for engineering plastics, namely those constructed from substituted benzene (e.g. polyethylene terephthalate), benzene-toluene-xylene (BTX) chemicals are vital [15]. In a cursory glance at the top chemicals derived from biomass, however, one sees a void in this category [16-19]. A renewable and direct source of aromatic-type chemical feedstock will address this important niche for the polymer community

Among possible biomass sources for BTX chemicals, a plant that appears interesting from a chemical standpoint is star anise (*Illicium verum*), whose essential oil is collected annually on a scale of 2,200 metric tons [20]. Found primarily in Guangxi province China (hardiness zone 10) [21], the plant is not a food source and only the leaves, fruits and flowers are harvested for the distillation process. The essential oil is routinely assayed at 90% or better *trans*-anethole (1-(4-methoxyphenyl)propene) and [22], because of its bifunctional nature, is a suitable 'phytofeedstock' for materials research in the engineering plastics realm. In searching for high-performance cyanate esters (aryl–O–C≡N) starting from renewable, chemical building blocks, we recently described results from diphenols obtained through dimerization of *trans*-anethole [23]. These dicyanates thermally polymerized to polycyanurate networks (Fig. 1) with high glass transition temperatures, excellent water resistance, and simple processing.

Drawing inspiration from the work of Lligadas et al. [24] with vegetable oils, this report describes the derivitization of *trans*-anethole to its dehydro or carbon–carbon triple bond analog (dehydroanethole), which by way of intermolecular [2+2+2] cycloaddition gave triphenols. The trisphenols were converted into tricyanate esters and readily cured into polycyanurate networks with low moisture uptake and glass transition temperatures of up to 362 °C, thus demonstrating that the improved thermo-mechanical performance of networks based on tricyanate esters (in comparison to those based on dicyanate esters) is available while preserving the low moisture uptake associated with anethole-based monomers. Also demonstrated is the somewhat surprising but very important discovery that in these uncatalyzed cyanate networks with a high glass transition temperature and low moisture uptake, the degradation in performance due to exposure to moisture is significantly reversible.
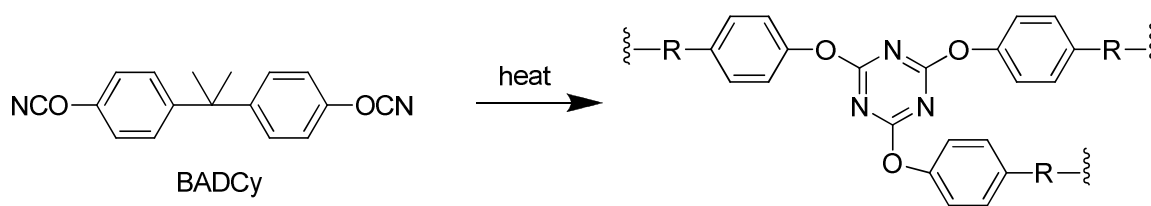
Figure 1. General reaction for polycyanurate network formation by heating dicyanate ester.

2. Experimental

2.1. Materials

The CoI$_2$ (95%), ZnBr$_2$ (98%), Zn dust (98%) cyanogen bromide (BrCN), pyridine, 5 % palladium on carbon (Pd/C), and phosphorus oxychloride (POCl$_3$) were purchased from Sigma-Aldrich (Milwaukee). *Trans*-anethole (> 98 %) was purchased from TCI America (Portland). All other reagents and solvents were obtained commercially and used as received.

2.2. Synthesis of monomers **5** and **9**

For complete experimental details of the synthesis of tricyanate monomers **5** and **9** refer to the Supplementary Data.

2.3. Thermal curing of monomers

Prior to cyclotrimerization, monomers were partially de-gassed along with a silicone mold for 30 minutes under reduced pressure (300 mm Hg) at a temperature of 10 – 20 °C above the melting point. If the melting point exceeded 150 °C, then only the silicone mold was de-gassed under 300 mm Hg at 150 °C for 30 minutes, and the monomer was melted as quickly as possible at 10 – 20 °C above the melting point. Each monomer was then poured into the mold and cured under flowing nitrogen for 1 hour at 150 °C followed by 24 hours at 210 °C to produce

void-free discs measuring approximately 13.7 mm in diameter and 1.6 mm thick and weighing 200-300 mg. The temperature ramp rate during cure was 5 °C/min. For monomers with melting points above 150 °C, the initial 1 hour hold at 150 °C was skipped. Note that no catalyst was added to any of the monomers. Cured discs were cut with a Struers Somotom-10 saw using a diamond-coated non-ferrous disc to produce surfaces with appropriate, reproducible roughness characteristics.

2.4. Conditioning of polycyanurate networks

For water uptake tests, some cured sample discs were placed in approximately 300 mL of deionized water at 85 °C for 96 hours. For weighing, samples were removed and their surfaces dried. Mass was measured before and after exposure.

2.5. Measurement and characterization

2.5.1. General methods

The melting points were collected on a Mel-Temp II from Laboratory Devices (Holliston, MA) and are not corrected. All NMR data were collected on a Bruker Avance II 300 MHz spectrometer. Nuclear magnetic resonance data (free-induction decay's) were processed using NUTS software from Acorn NMR (Livermore, CA). All spectra are referenced to solvent or tetramethylsilane. Elemental analyses were performed by Atlantic Microlab, Inc. (Norcross, GA).

2.5.2. Fourier transform infrared analyses

Fourier transform infrared spectroscopy (FT-IR) was carried out using a Thermo Corporation Nicolet 6700 spectrometer in attenuated total reflectance mode with the ZnSe crystal

attachment. A total of 512 scans were completed on these surfaces with a resolution of 4 cm^{-1} to obtain spectra. The integrated area between 1480 cm^{-1} and 1510 cm^{-1}, containing the aromatic ring peak near 1500 cm^{-1}, was used for normalization, with a quadratic baseline determined by using 1810 cm^{-1}, 2100 cm^{-1}, and 2500 cm^{-1} as zero points.

2.5.3. Density measurement

The density of the cured resins was determined by placing cured discs in solutions of CaCl$_2$ (as the dihydrate) and deionized water and varying the CaCl$_2$ concentration until neutral buoyancy was observed on bubble-free samples over a period of several minutes. The density of the neutrally buoyant solution was determined by placing 10.00 mL in a volumetric flask (calibrated with deionized water at 20 °C) and weighing, and checked against the predicted density of the solution at ambient temperature based on the known concentration of CaCl$_2$.

2.5.4. Thermal analysis

2.5.4.1. Differential scanning calorimetry

Differential scanning calorimetry (DSC) was performed on ~10 mg of monomer reserved after de-gassing using a TA Instruments Q2000 calorimeter under 50 mL/min. of flowing nitrogen. Samples were heated to 350 °C, then cooled to 100 °C and re-heated to 350 °C, all at 10 °C/min. The same protocol was also carried out on ~10 mg fragments of cured discs.

2.5.4.2. Oscillatory thermomechanical analyses

Cured discs were also tested via oscillatory thermomechanical analysis (OTMA) with a TA Instruments Q400 series analyzer under 50 mL/min of nitrogen flow. The discs were initially held in place with a compressive force of 0.2 N using the standard ~5 mm diameter flat

cylindrical probe. The force was then modulated at 0.05 Hz over an amplitude of 0.1 N (with a mean force of 0.1 N) and the temperature was ramped twice (heating and cooling) between 0 °C and 200 °C (to aid in determination of thermal lag) followed by heating to 350 °C, cooling to 100 °C, and re-heating to 350 °C, all at 50 °C/min. For samples previously exposed to hot water, the heating rate was decreased to 20 °C/min and the order of segments were: heating to 350 °C, cooling to 100 °C, two cycles between 100 °C and 200 °C for thermal lag determination, and finally heating to 350 °C. The details of the thermal lag determination procedure have been reported elsewhere [25].

2.5.4.3. Thermogravimetric analyses

Thermogravimetric analysis (under both nitrogen and air) was performed on ~10 mg samples of cured discs, using a TA Instruments Q5000 analyzer, at a gas flow rate of 10 mL/min (balance) and 25 mL/min (purge), heating the samples at 10 °C/min to 600 °C.

3. Results and discussion

3.1. Synthesis of monomers

For expediency, the two-step process of bromination/dehydrobromination used by Gramatica et al. [26] was chosen as the method to effect oxidation of *trans*-anethole (**1**) to dehydroanethole (**2**) (Scheme 1) [27,28]. Typical conditions for bromination of **1** use an unreactive solvent such as chlorinated hydrocarbons that give a diastereomeric mixture of vicinal dibromides [29-32]. Tetrahydrofuran (THF) has rarely been employed as a solvent for bromination of alkenes [33], most likely due to the possibility of forming a charge transfer complex like that of the stable solid $Br_2 \cdot 1,4$-dioxane [34]. The bromination of **1** was found to work well using THF as solvent at 0 °C requiring only a slight excess of bromine to achieve completion based on ^{1}H NMR

analysis of the reaction mixture. Therefore, rather than isolate the mixture of vicinal dibromide isomers, the reaction mixture was added to a solution of potassium *tert*-butoxide in THF which smoothly brought about double dehydrobromination to give the alkyne **2** [35-38]. This combination of reactions saved time yet did not effect much loss in overall yield (92%).
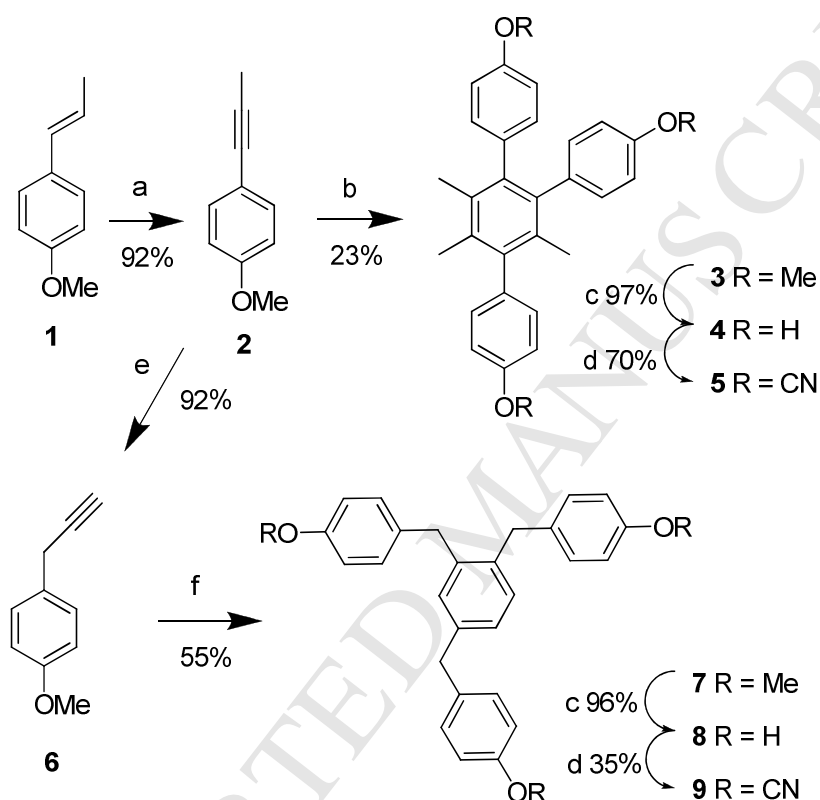
Reagents & conditions: a) 1. Br$_2$, THF, 0 °C; 2. KO*t*Bu, THF, 0 °C to reflux; b) TMSCl, 5% Pd/C, dioxane, reflux; c) pyridine, POCl$_3$, H$_2$O, reflux; d) BrCN, TEA, acetone, -20 °C; e) BuLi, Et$_2$O, hexanes, rt; f) CoI$_2$, ZnBr$_2$, Zn, MeCN; g) pyridineHCl, reflux.

Scheme 1. Synthetic route for tricyanate esters **5** and **9** from *trans*-anethole (**1**).

Since the discovery by Reppe [39,40] that soluble transition metal complexes can catalyze the intermolecular [2+2+2] cycloaddition of alkynes, there has been a steady increase in this transformation over the past 50 years [41-47]. With dehydroanethole (**2**) in hand, the conditions

for cyclotrimerization of Jianghan and Maier (Pd/C, trimethylsilyl chloride) [48] were carried out though using 1,4-dioxane at reflux to speed up the reaction. The product was a mixture of the 1,2,4-regioisomer **3** and its symmetrical isomer in a 3:1 ratio, respectively [49]. Fortunately, **3** could be separated by fraction crystallization. Demethylation of **3** was accomplished by refluxing in a previously prepared mixture of pyridine, water, and phosphorus oxychloride (3:3:1 ratio respectively). The resulting triphenol **4** was reacted under typical cyanation conditions (cyanogen bromide, triethylamine, acetone, - 20 °C) [50] to give the tricyanate ester **5** in an overall yield of 14%. Tricyanate **5** had a rather high melting point (T_m) of 165 °C (329 °F). The symmetrical isomer from this cycloaddition reaction was anticipated to make a tricyanate ester with an even higher melting point making curing and processing difficult (*vide infra*) and, therefore, was not pursued [51].

Ideally a liquid tricyanate ester was desired but one with a melting point less than 100 °C would be satisfactory and so further chemistry was explored. It is well known that 1-arylpropynes can be isomerized by strong base resulting in 3-arylpropynes, an interesting transformation proceeding through an allene intermediate [52-57]. Although the reaction was slow, compound **2** was efficiently isomerized to **6** following the conditions of Mulvaney et al.[58] though it was found critical to keep the reaction mixture cold during the water work-up for best yield (Scheme 1). The [2+2+2] cycloaddition of the parent 3-phenylpropyne had been studied previously by Choi et al. [59] and Rüba et al. [60] using metal catalyst ZrCl₄/Li and [RuCp(CH₃CN)₃]PF₆, respectively, each leading to ~3:1 mixtures favoring the unsymmetrical tribenzylbenzene isomer. So it was anticipated that cycloaddition would be successful with **6,** at least with those catalysts, but it was decided to explore the convenient, "instant" cobalt catalyst system developed by Hilt's group [61-65]. Reaction of **6** with CoI₂/Zn/ZnBr₂ in acetonitrile,

without any triarylphosphine or 1,2-diimine ligand, gave a crude product mixture of cyclotrimer **7** and symmetrical isomer in a 19:1 ratio, respectively, based on integration of the CH_2 peaks in ^{13}C NMR.   Owing to this remarkably selective reaction, product **7** was purified by recrystallization in a yield of 55%.   Indeed, the reaction is also interesting for the fact that the solvent, with an sp-hybridized bond, did not participate in the cycloaddition reaction which has been demonstrated with cobalt and other catalysts [66-68].   Tricyanate ester **9** was then made from **7** in 15% overall yield by a similar three-step sequence of reactions mentioned above in the synthesis of **5**, in this case using commercial pyridine hydrochloride.   Tricyanate **9** had a T_m of 85 °C (185 °F) and so too were intermediates **7** and **8** solids, but despite significant effort, appropriate solvent/conditions for X-ray quality crystals of these compounds, to provide further support for these structures, was not found.   The ^1H and ^{13}C NMR spectra of **9** clearly show the unsymmetrical nature of the molecule, for example the individual methylene peaks and complex aromatic region (Fig. S1, Supplementary Data).   Unfortunately, without a more powerful NMR instrument, the three individual cyanate resonances of **9** overlap in the ^{13}C spectrum.

3.2. Synthesis of polycyanurates and characterization

Analysis of monomer **5** by differential scanning calorimetry (DSC) (Fig. 2) showed the main polymerization exotherm began shortly after melting.   Unfortunately, potential thermosetting monomers that do not provide an adequate temperature range between the melting point and the onset of rapid gelation, the so-called processing window (*vide infra*), are not useful for molding operations [69,70].   Therefore, monomer **9** with its greater degree of conformational freedom and lower melting point, became the focus of our attention. Analysis of monomer **9** by DSC (Fig. 3) shows good baseline separation between melting and the main polymerization (or cure) exotherm peak commencing at ∼ 200 °C, which is typical of cyanate esters.   The total heat

output of the exothermic event was 620 J/g alternately expressed as 97 kJ/cyanate ester, a more

convenient value with which to compare different cyanate esters (Table 1). The 97 kJ/cyanate

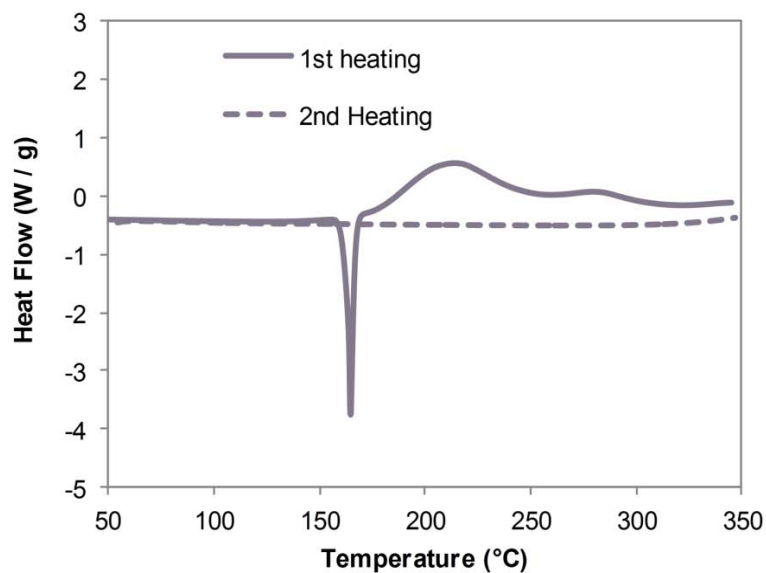ester is a typical value seen in other cyanate esters and represents near complete cure.
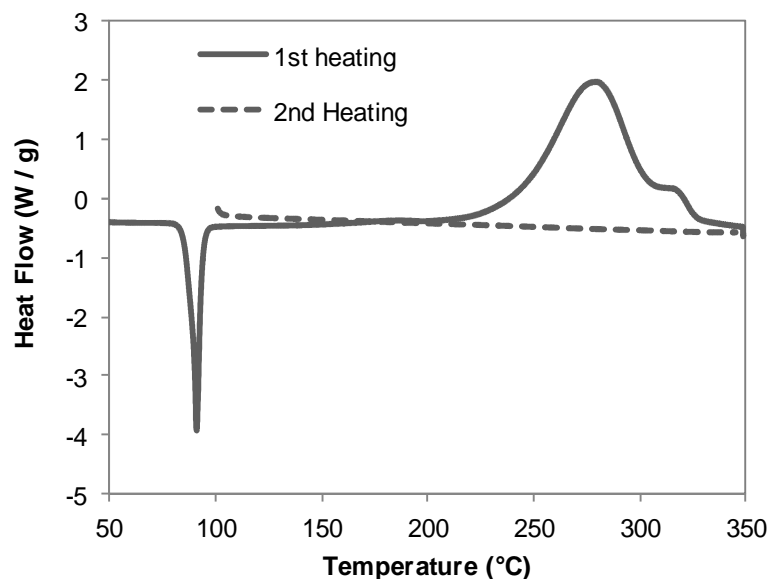

Figure 2. DSC trace of monomer **5**.

Figure 3. DSC trace of monomer **9**.

A mild cure schedule of 150 °C for 1 hour followed by 210 °C for 24 hours was used to prepare sample discs for further testing. By this heating protocol, curing of **9** produced a high conversion, as evidenced by Fourier transform infrared (FTIR) analysis which showed some residual cyanate stretch at 2250 cm^{-1} and strong peaks at 1360 and 1570 cm^{-1} corresponding to triazine (Fig. S2, Supplementary Data) [71]. A DSC scan of a small chip from the cured disc (Fig. 4) indicates a residual cure amounting to 19 ± 2 kJ/eq, with the onset of residual cure preceded by what appears to be a glass transition temperature (T_g) of around 235 °C. Since the T_g signals for polycyanurate networks can sometimes be very broad [72] while the signal in Fig. 4 appears narrow and truncated, a confirmatory indication of the "as cured" T_g was sought. An oscillatory thermomechanical analysis (TMA) trace (Fig. S3, Supplementary Data) showed that under this cure schedule polycyanurate **9** exhibited a T_g of 277 °C (tan δ peak). Despite the use of a very rapid heating rate (50 °C / min.), this higher T_g likely reflects the effects of some *in-situ* cure during the analysis experiment. After continued heating to 380 °C to achieve full cure, the

oscillatory TMA experiments clearly show T_g of 362 °C (DSC scans at these temperatures are significantly affected by slight decomposition of the network, whereas signals from mechanical methods are minimally affected).
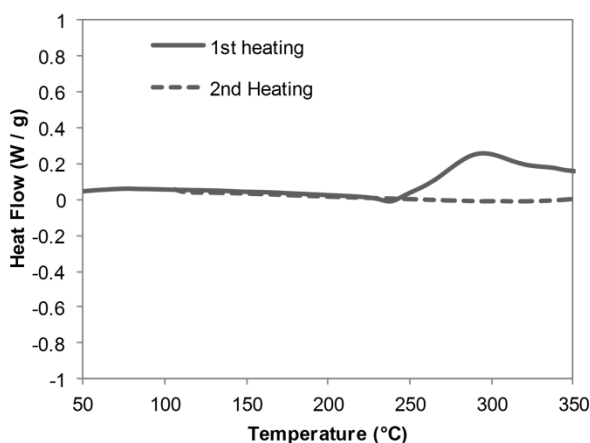

Figure 4. DSC of **9**, after curing at 210 °C for 24 hours.

The determination of the T_g at full cure provides the key parameter needed for use of the diBenedetto equation [73,74] to relate the T_g to the extent of cure in polycyanurate networks. As described in the Supplementary Data, data for the diBenedetto equation was generated using partially cured samples prepared in the DSC, and a good fit with a typical value for the parameter λ of 0.44 ± 0.06 was obtained. The diBenedetto equation predicts that a polycyanurate network cured from **9** with a residual exotherm of 19 kJ/eq. will exhibit a T_g of 240 ± 7 °C, corresponding to the location of the probable T_g seen in the Fig. 4.

Reduction in mechanical and physical properties (e.g. reduction of T_g, swelling) of polycyanurate networks can be linked to absorption of moisture and plasticization and/or chemical alteration of the polymer matrix [75,76]. To examine this effect, a sample of **9** cured for 24 hours at 210 °C was subjected to hygrothermal ageing by exposure to hot water (85 °C).

After 96 hours the sample had water uptake of only 1.4 wt%. This water challenged sample was analyzed again by oscillatory TMA (Fig. 5) which showed two peaks at 187 °C and 303 °C in the loss modulus curve.
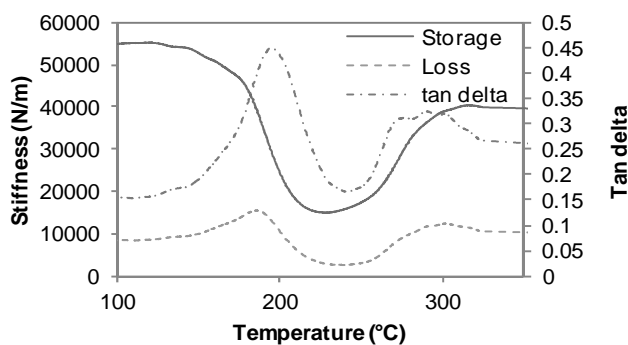

Figure 5. TMA of cured **9** after exposure to 85 °C water for 96 hours.

In order to better understand the behavior observed in Fig. 5, a similarly-cured sample of **9** (conversion 87%, dry "as cured" T_g 270 °C) was tracked via FT-IR, DSC, TMA, and weight gain measurements during the course of exposure to 85 °C water for 96 hours followed by heating to 350 °C in the TMA. The heating run was interrupted when the temperature set point reached 200 °C, the sample was weighed, and a portion of the sample was removed for DSC and FT-IR testing; the remainder was then returned to the TMA and the heating run continued. In this manner, the effects of water exposure, heating below the first "wet" T_g, and subsequent heating could be determined separately.

Figure 6 shows the FT-IR traces of the sample "as cured", exposed to water (but not subsequently heated), and exposed with re-heating to 200 °C and 350 °C. Additional views showing the key peaks for cyanurate (1360 and 1555 cm^{-1}), cyanate ester (2200-2300 cm^{-1}), carbamate (1720 cm^{-1}), and phenol (1600 cm^{-1}) are available in Supplementary Data (Figs. S6

and S7). Integration of the relevant peaks revealed that around 35% of the cyanate ester groups (or 5 mol% of the cyanate ester groups originally present in the monomer) disappeared on exposure to water, with the appearance of a significant carbamate peak and little change in the cyanurate peaks. The simplest explanation is that residual cyanate ester groups are converted to carbamate on exposure to water, that heating to 200 °C does not produce further carbamate groups due to insufficient available time, and that carbamate groups decompose after heating to 200 °C. This explanation matches the generally accepted picture of the formation and destruction of carbamate groups in cyanurate networks [77-81].
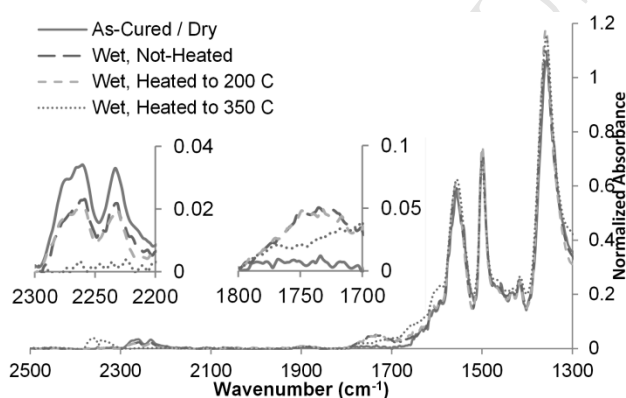

Figure 6. FT-IR scans of cured **9** at various points before, during, and after exposure to 85 °C water and subsequent heating.

Moreover, the weight change data indicates a gain of 2.4% on exposure to water. (This value is higher than the sample with 80% conversion due to the strong increase in water uptake with increasing conversion in cyanurate networks, combined with the effect of curing well below T_g (increases water uptake) as opposed to near T_g.) The weight then decreases by 0.4% (original weight basis) on heating to 200 °C, presumably due to some loss of water of plasticization, followed by a further decrease of 2.4% (net mass loss of 0.4% compared to original sample mass) on heating to 350 °C. These data are consistent with reversible water uptake, formation of

roughly 5 mol carbamate per 100 mol of uncured cyanate ester on exposure to water (as indicated by FT-IR), subsequent decomposition of carbamate with release of CO_2 when heated above 200 °C, and little or no permanent weight gain due to hydrolysis of cyanurate ring structures.

Additional details may be inferred by examining the corresponding DSC traces (Fig. 7). As in Fig. 4, both the extent and onset temperature of residual cure in the "as cured" sample match the expected behavior for a network with a T_g of 270 °C. After exposure to water and heating to 200 °C, the exotherm shifts to lower temperatures (an indication of a significant drop in T_g) and, despite the loss of roughly 35% of the uncured cyanate ester groups, the residual enthalpy increases, at 82 ± 6 J/g before exposure to 117 ± 23 J/g after exposure and heating to 200 °C. A DSC scan of the sample after exposure to water and heating to 350 °C in a TMA experiment shows only a broad residual enthalpy (using the subsequent re-scan as a baseline). These results clearly indicate that exposure to water induces additional chemistry on subsequent heating to 350 °C not seen in dry samples, with carbamate decomposition being the most likely candidate.
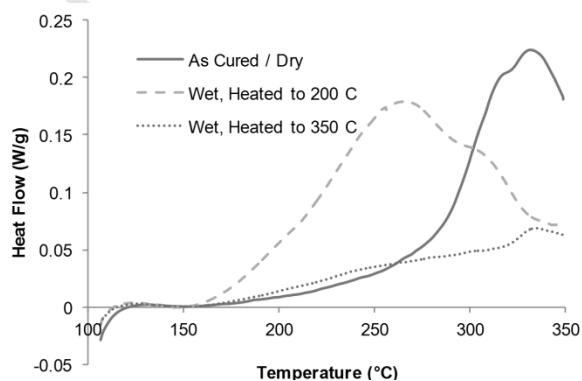
Figure 7. DSC scans (1st heating) of cured **9** at various points before, during, and after exposure to 85 °C water and subsequent heating, with the baseline (based on a 2nd heating scan) subtracted.

A further bit of information may be obtained by comparing the second scans of the aforementioned DSC traces. These second scans are shown in Fig. 8. Each of these samples has been previously heated to 350 °C, but via different paths. The "as cured" sample has not been exposed to water, and the "heated to 200 °C" and "heated to 350 °C" samples have been heated as indicated in the TMA as well as being re-heated to 350 °C in the DSC. Exposure to 350 °C is expected to remove any uncured cyanate ester groups either by conversion to cyanurate or thermal decomposition, and to decompose any carbamate groups.
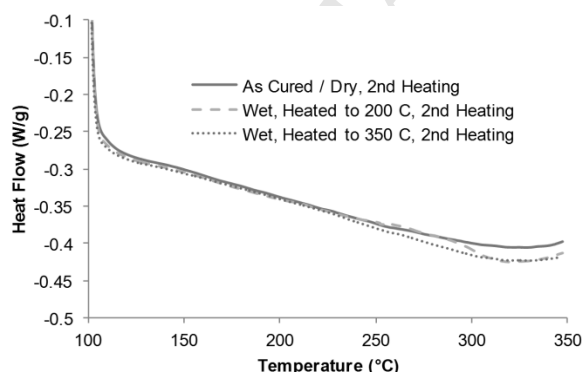

Figure 8. DSC scans (2nd heating) of cured **9** at various points before, during, and after exposure to 85 °C water and subsequent heating. The curves have been offset to coincide at low temperatures, in order to make the broad glass transitions more apparent.

Despite having all been heated to 350 °C at least once, the samples show different T_g characteristics. The "as cured" sample shows no T_g, presumably because a fully-cured network

has formed with an expected T_g of 362 °C, which is too high to appear in the scan. The sample exposed to water but heated only to 200 °C in the TMA shows a clearly defined T_g around 300 °C, indicating a lower density of cross-links. Because roughly 5 mol% of the original cyanate ester groups have been converted to carbamates and decomposed in this sample, these groups may be unavailable to form cross-links and instead form dangling chain ends, depressing the T_g even after all remaining cyanate ester groups have reacted to form cross-links. The sample heated to 350 °C in the TMA shows a broad T_g of 250 – 300 °C, in agreement with the T_g value of 260 °C seen in the TMA scan itself (all data from the TMA scans is shown in Supplementary Data, Figures S8-S10). The sample heated to 350 °C in the TMA thus shows a lower and broader T_g than the sample heated to only 200 °C in the TMA and 350 °C in the DSC. The DSC sample is comprised of a ~5 mg chip while the TMA sample consists of a ~300 mg disc. Both are exposed to a similar 50 mL/min. flow of dry nitrogen, but due to the smaller sample size, drying will be much faster in the DSC sample. Retained moisture in the TMA sample therefore likely causes increased conversion of residual cyanate ester groups to carbamates followed by decarboxylation above 200 °C [82]. This effect also helps explain the differences in the "wet" TMA scans in the two samples of cured **9** studied. For the sample with 81% conversion and a low moisture uptake of just 1.4%, fewer residual cyanate ester groups will be lost, allowing for greater recovery of T_g on heating due to *in-situ* cure (the dual peaks in the TMA scan are characteristic of such *in-situ* cure) [83].

As previously mentioned, exposure of cyanurate networks to hot water has traditionally been expected to result in an irreversible decline in T_g, though at least one exception has been reported [84]. Previous studies of carbamate formation in cyanate esters [79] have shown that the rate of carbamate formation may be changed by at least an order of magnitude depending on

the type and level of catalyst used. Similarly dramatic effects on the rate of T_g decline as a function of catalyst level and type have been reported for cyanate esters based on polyphenolic resins [85]. Although concrete experimental data is lacking, it is also reasonable to assume that the rate of degradation will be proportional (though perhaps not linearly) to the concentration of absorbed water. Because the performance of cyanurate networks is more commonly studied using catalyzed systems, because most cyanurate networks absorb more water than **9**, and because most cyanurate networks achieve a higher degree of conversion than **9** during typical cure (due to a lower T_g), the conditions employed in the analysis of cured **9** are unusually favorable for the recovery of T_g. The fact that recovery has been demonstrated, however, and the elucidation of the conditions under which it is likely to occur, represent an important advance in the study of cyanurate networks. These results also indicate that, if a sufficiently active cure catalyst that does not simultaneously promote hydrolysis can be identified and utilized, then very significant improvements in the performance of cyanurate networks in terrestrial applications can be achieved.

Contextualization of the thermal analysis data of the bio-derived tricyanate ester **9** was made with that from two cyanate esters derived wholly from petroleum sources, the tricyanate ester **10** (Fig. 9) and the commercial dicyanate of bisphenol A (BADCy) [86] (Tables 1 and 2). The data for the latter compounds was taken largely from our previous reports [23,87]. Interestingly, tricyanate **10,** though prepared by a completely different synthetic route, is the symmetrical isomer of tricyanate **9**. The DSC data for tricyanates **9** and **10** are almost identical (cure onset T and ΔH) which is understandable considering the slight difference in chemical structure (Table 1). Owing to its asymmetric shape [51], tricyanate **9** has a melting point 12 °C

lower than its symmetrical counterpart, and almost the same as BADCy which is significant for molding operations.
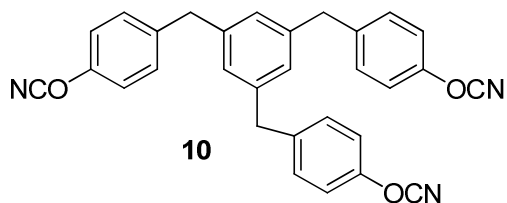

Figure 9. Isomeric tricyanate ester **10** previously prepared from petrochemical starting materials.

Table 1

Comparison of DSC data for monomers **5**, **9**, **10** and BADCy

Compound	T_m (°C)	Cure Onset (°C)	Exotherm Max (°C)	ΔH_{cure} (J/g)	ΔH_{cure} (kJ/cyanate ester)
5	165	170	215	600	54
9	85	225	280	620	97
10	97	230	280	780	123
BADCy	82	270	330	810	108

According to Table 2, after full cure, the T_g of polycyanurate **9** is ~ 40 °C higher than the polycyanurates of BADCy and 20 °C higher than **10**. Both water uptake and density of cured BADCy, **9**, and **10** are strongly correlated to cyanate ester conversion. The higher density and lower water uptake of **9** compared to **10** are the result of both lower conversion in **9** and the relative similarity of the cure temperature (210 °C) and the "as cured" T_g. When cured near T_g, the free volume (or unoccupied space between molecules created by the decrease in Van der Waals volume as conversion increases) is able to disappear via physical relaxation, leading to

higher density and lower uptake, whereas when the cure temperature is below T_g, the free volume remains frozen in place. These phenomena have been confirmed by positron annihilation studies in BADCy [88].

Table 2

Comparison of key thermomechanical analysis data of cured **9**, **10** and BADCy

Compound	Density (g/mL)	Cyanurate Density at Full Cure (mmol/mL)	As-Cured Dry T_g (°C)	T_g 350 °C Post-Cure (°C)	"Wet" T_g (°C)	Water Uptake (wt%)
9	1.23	2.61	277	362	303	1.35
10	1.17	2.48	280	338	238	2.2
BADCy	1.21	2.89	275	323	240	1.34
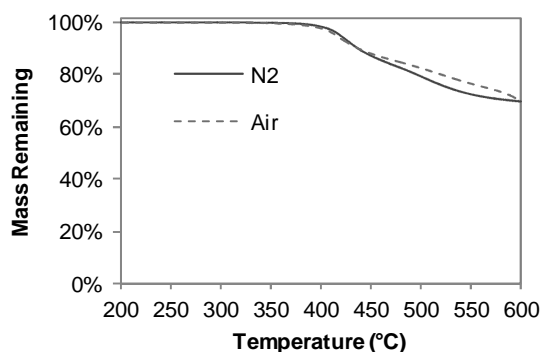
Figure 10. TGA traces of polycyanurate **9**.

The thermogravimetric analysis (TGA) curve up to 600 °C for **9** in both nitrogen and air atmospheres is shown in Fig. 10 and key data is compared with **10** and BADCy in Table 3. The thermal stability of **9** is only slightly less than **10** (Fig. S4, Supplementary Data), but **9** loses more mass in the initial degradation step. Polycyanurate **9** is more stable that BADCy, however, with char yields in nitrogen and air that are 20% and 50% higher, respectively. This is most

likely due to the thermal lability of quaternary aliphatic carbon content which is absent in **9** and **10** [89].

Table 3

Comparison of TGA data for cured **9**, **10** and BADCy

| Compound | T @ 5% weight loss (°C) | | Char Yield 600 °C (%) | | % weight loss @ T (°C) | | | | | |
	N_2	Air	N_2	Air	N_2 450	550	600	Air 450	550	600
9	419	415	69	70	13	15	3	12	11	7
10	449	443	77	75	5	12	6	7	13	5
BADCy	402	400	47	25	35	15	3	37	13	25

4. Conclusions

Novel bio-based tricyanate esters **5** and **9** were prepared from the natural product *trans*-anethole by way of [2+2+2]-cycloaddition. Tricyanate **9**, with more conformational flexibility and lower melting temperature gave a wide processing window of at least 100 °C and could be cured to polycyanurate with thermal properties in the realm of high-performance polymers. The new bio-based tricyanate **9** had T_g (~ 362 °C at full cure), water uptake (1.4-2.4 %) and T_m (85 °C) equal or better in all respects to the petrochemical-based BADCy and could make a 'drop in' replacement for the latter. When cure far below T_g is avoided, so as to keep moisture uptake low, the uncatalyzed cured **9** demonstrated the unexpected ability to significantly recover thermo-mechanical performance after hygrothermal exposure, a discovery with significant potential technological importance for cyanurate networks in general. Tricyanate **9** and its isomer **10** were very close in their thermal parameters and both had better thermal stability and higher char yields than BADCy. *Trans*-anethole appears to be versatile molecule with which to

generate polyphenols and we hope to synthesize and characterize a variety of other polymer systems (e.g., epoxy, polycarbonate, polyester, etc.) from them in the future.

Acknowledgements

Appendix. Supplementary data

Supplementary data associated with this article can be obtained free of charge, in the online version, at XXXXX

References

[1] Hubbert MK, Nuclear Energy and the Fossil Fuels. Publication No. 95, Shell Development Company, Exploration and Production Research Division, Houston, Texas, 1956.

[2] Meadows DH, Meadows DL, Randers J, Behrens III WW. Limits to Growth: a Report for the Club of Rome's Project on the Predicament of Mankind. New York: Universe Books; 1972.

[3] Heinberg R. The Party's Over: Oil, War, and the Fate of Industrial Societies. British Columbia: New Society Publishers; 2003.

[4] Campbell CJ, Laherrère JH. Sci Am 1998;278:78-83.

[5] Sherwood M. New Sci 1973;60:777-8.

[6] Komiyama R, Li Z, Ito K. Int J of Global Energy Issues 2005;24:183-210.

[7] United Nations. World Population Prospects: The 2002 Revision. New York; 2003.

[8] Plant/crop-based renewable resources 2020: A vision to enhance U.S. economic security through renewable plant/crop-based resource use. US Department of Agriculture; 1998 January Report No. DOE/GO-10097-385.

[9] Armstrong RE. From Petro to Agro: Seeds of a New Economy. Center for Technology and National Security Policy, National Defense University. Washington (DC): Government Printing Office; 2002.

[10]   Wang SC, Huffman JB. Econ Bot 1981;35:369-82.

[11]   Lipinsky ES. Science 1981;212:1465-71.

[12]   Karger-Kocsis J. Express Polym Lett 2009;3:676.

[13]   Calvin M. Bioscience 1979;29:533-8.

[14]   Dijkstra DJ, Langstein G. Polym Int 2012;61:6-8.

[15]   Szmant HH. Organic building blocks of the chemical industry. New York: John Wiley & Sons; 1989.

[16]   Corma A, Iborra S, Velty A. Chem Rev 2007;107:2411-502.

[17]   Werpy T, Peterson G, editors. Top value-added chemicals from biomass, volume I: results from screening for potential candidates from sugars and synthesis gas. US Department of Energy. Washington (DC): Government Printing Office; 2004.

[18]   Holladay JE, Bozell JJ, White JF, Johnson D. Top value-added chemicals from biomass, Volume II: results of screening for potential candidates from biorefinery lignin. Pacific Northwest National Laboratory Report No. 16983. Washington (DC): Government Printing Office; 2007.

[19]   Christensen CH, Rass-Hansen J, Marsden CC, Taarning E, Egeblad K. ChemSusChem 2008;1:283-9.

[20]   Consultative Group on International Agricultural Research. China: voices for sustainable agriculture. Washington (DC); 2007. p 14-7.

[21]   Hardiness zones in China. [climate map]. Ames: US Department of Agriculture-Agricultural Research Service, Iowa State University; 1997.

[22]   Environmental Protection Agency. Test plan for anethole (isomer unspecified) and trans-anethole. Washington (DC); 2002.

[23]   Davis MC, Guenthner AJ, Groshens TJ, Reams JT, Mabry JM. J Polym Sci Part A: Polym Chem 2012;50:4127-36.

[24]   Lligadas G, Ronda JC, Galia M, Cádiz V. Biomacromolecules 2007;8:1858-64.

[25]   Guenthner AJ, Yandek GR, Mabry JM, Lamison KR, Vij V, Davis MC, Cambrea LR. Insights into moisture uptake and processability from new cyanate ester monomer and blend studies. SAMPE International Technical Conference, vol. 55. Salt Lake City, UT: SAMPE International Business Office; 2010. p. 42ISTC-119.

[26]   Gramatica P, Monti D, Manitto P. Gazz Chim Ital 1974;104:629-32.

[27]   Orita A, Otera J. Chem Rev 2006;106:5387-412.

[28]   Naves Y–R. Helv Chim Acta 1960;43:230-2.

[29]   McGahey L. J Chem Educ 1990;67:554-5.

[30]   Arrieta A, Ganboa I, Palomo C. Synth Commun 1984;14:939-45.

[31]   Fahey RC, Schneider H–J. J Am Chem Soc 1968;90:4429-34.

[32]   Hell C, von Günther O. J Prakt Chem 1895;52:193-210.

[33]   Kunitake T, Aso C, Ito K. Makromol Chem 1966;97:40-8.

[34]   Metsger L, Bittner S. Tetrahedron 2000;56:1905-10.

[35]   Grob CA, Nussbaumer R. Helv Chim Acta 1971;54:2528-35.

[36]   Taherirastgar F, Brandsma L. Synth Commun 1997;27:4035-40.

[37]   Krause M, Ligneau X, Stark H, Garbarg M, Schwartz J–C, Schunack W. J Med Chem 1998;41: 4171-6.

[38]   Schulze K, Mühlstädt M. J Prakt Chem 1966;33:84-95.

[39]   Reppe W, Schwekendiek WJ. Justus Liebigs Ann Chem 1948;560:104-16.

[40]   Rose JD, Statham FS. J Chem Soc 1950:69-70.

[41]   Kotha S, Brahmachary E, Lahiri K. Eur J Org Chem 2005:4741-67.

[42]   Frühauf H–W. Chem Rev 1997;97:523-96.

[43]   Chopade P R, Louie J. Adv Synth Catal 2006;348:2307-27.

[44]   Domínguez G, Pérez-Castells J. Chem Soc Rev 2011;40:3430-44.

[45]   Broere DLJ, Ruijter E. Synthesis 2012;2639-72.

[46]   Galan BR, Rovis T. Angew Chem Int Ed Eng 2009;49:2830-34.

[47]   Schore NE. Chem Rev 1988;88:1081-119.

[48]   Jhingan AK, Maier WF. J Org Chem 1987;52:1161-5.

[49]   Rodríguez JG, Lafuente A, Martín-Villamil R. J Polym Sci Part A: Polym Chem
2005;43:5987-97.

[50]   Grigat E, Pütter R. Chem Ber 1964;97:3012-7.

[51]   Slovokhotov YL, Neretin IS, Howard JAK. New J Chem 2004;28:967-79.

[52]   Lawson KR, inventor; Imperial Chemical Industries PLC, assignee; Pyrimidine
compounds. US Patent 5,090,992. 1992 Feb 25.

[53]   West R, Gornowicz GA. J Am Chem Soc 1971;93:1720-4.

[54]   Klein J, Brenner S. J Org Chem 1971;36:1319-20.

[55]   Brandsma L, Mugge E. Recl Trav Chim Pays-Bas 1973;92:628-30.

[56]   Maercker A, Fischenich J. Tetrahedron 1995;51:10209-18.

[57]   Newman-Evans RH, Simon RJ, Carpenter BK. J Org Chem 1990;55:695-711.

[58]   Mulvaney JE, Folk TL, Newton DJ. J Org Chem 1967;32:1674-5.

[59]   Choi KS, Park MK, Han BH. Bull Korean Chem Soc 1998;19:1257-61.

[60]   Rüba E, Schmid R, Kirchner K, Calhorda MJ. J Organomet Chem 2003;682:204-
11.

[61]   Doszczak L, Fey P, Tacke R. Synlett 2007:753-6.

[62]   Lombardo M, Pasi F, Trombini C, Seddon KR, Pitner WR. Green Chem 2007;9:321-2.

[63]   Hilt G, Weiss W, Vogler T, Hengst C. J Organomet Chem 2005;690:5170-81.

[64]   Saino N, Amemiya F, Tanabe, E, Kase K, Okamoto S. Org Lett 2006;8:1439-42.

[65]   Slowinski F, Aubert C, Malacria M. Adv Synth Catal 2001;343:64-7.

[66]   Wakatsuki Y, Yamazaki H. Tetrahedron Lett 1973;14:3383-4.

[67]   Wakatsuki Y, Nomura O, Kitaura K, Morokuma K, Yamazaki H. J Am Chem Soc 1983;105:1907-12.

[68]   Bönnemann H, Brinkmann R, Schenkluhn H. Synthesis 1974:575-577.

[69]   Rimdusit S, Jubsilp, C, Kunopast P, Bangsen W. Chemorheology of benzoxazine-based resins. In: Ishida H, Agag T, editors. Handbook of Benzoxazine Resins. Amsterdam: Elsevier; 2011.

[70]   Halley PJ, Mackay ME. Polym Eng Sci 1996;36:593–609.

[71]   Ramirez ML, Walters R, Savitski EP, Lyon RE. Thermal Decomposition of Cyanate Ester Resins. Report# AR01/32. Washington: US Department of Transportation, Federal Aviation Administration; 2001.

[72]   Earnest CM. Assignment of glass transition temperatures using thermomechanical analysis. In: Seyler RJ, editor.   Assignment of Glass Transition, ASTM STP 1249. Philadelphia: American Society for Testing and Materials; 1994.

[73]   Simon SL, Gillham JK. J Appl Polym Sci 1993;47:461-85.

[74]   Sheng X, Akinc M, Kessler MR. J Therm Anal Calorim 2008;93:77-85.

[75]   Fuzek JF. Glass transition temperature of wet fibers: its measurement and significance. In: Rowland SP, editor. Water in Polymers. ACS Symposium Series, Vol. 127. Washington (DC): American Chemical Society; 1980.

[76]   Morgan RJ, Shin, EE, Drzal, LT, Lee A. Characterization of Critical Fundamental Aging Mechanisms of High Temperature Polymer Matrix Composites. Report# AFRL-SF-BL-TR-00-0262. Arlington: Air Force Office of Scientific Research; 1998.

[77]   Chaplin A, Hamerton I, Herman H, Mudhar AK, Shaw SJ. Polymer 2000;41:3945-56.

[78]   Micro V, Méchin F, Pascault J-P. Proc ACS Div Polym Mater Sci Eng 1994;71:688-9.

[79]   Shimp DA, Ising SJ. Proc ACS Div Polym Mater Sci Eng 1991;66:504-5.

[80]   Grigat E, Pütter R. Angew Chem Int Ed 1967;6:206-18.

[81]   Georjon O, Galy J, Pascault J-P. J Appl Polym Sci 1993;49:1441-52.

[82]   Hamerton I. Properties of unreinforced cyanate ester matrix resins. In: Hamerton I. editor. Chemistry and technology of cyanate ester resins. Glasgow: Blackie A&P; 1994.

[83]   Guenthner AJ, Lamison KR, Yandek GR, Masurat KC, Reams JT, Cambrea LR, Mabry JM. Abstr. Pap. Am. Chem. Soc. 2011, p. 242.

[84]   Amarillas M. Wet Tg Determination of high temperature composites using DMA. Paper presented at the 37th Annual Conference of Thermal Analysis and Applications; 2009 Sept 20; Lubbock (USA).

[85]   Marella VV. An Investigation of the Hydrolysis of Polyphenolic Cyanate Esters using Near-IR Spectroscopy [dissertation]. Philadelphia: Drexel University; 2008.

[86]   Vandenberg LN, Maffini MV, Sonnenschein C, Rubin BS, Soto AM. Endocr Rev
2009;30:75-95.

[87]   Guenthner AJ, Davis MC, Ford MD, Reams JT, Groshens TJ, Baldwin LC, et al.
Macromolecules 2012;45:9707-18.

[88]   Georjon O, Galy J. Polymer 1998;39:339-45.

[89]   LaMarca C, Libanati C, Klein MT, Cotter RJ, Andrews SM. ACS Div Fuel Chem
Preprints 1991;36:676-82.
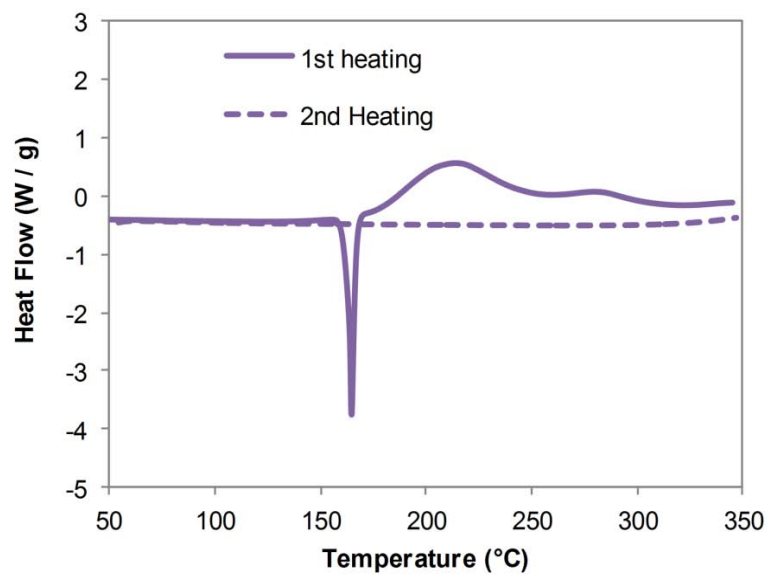
Figure 2. DSC trace of monomer **5**.
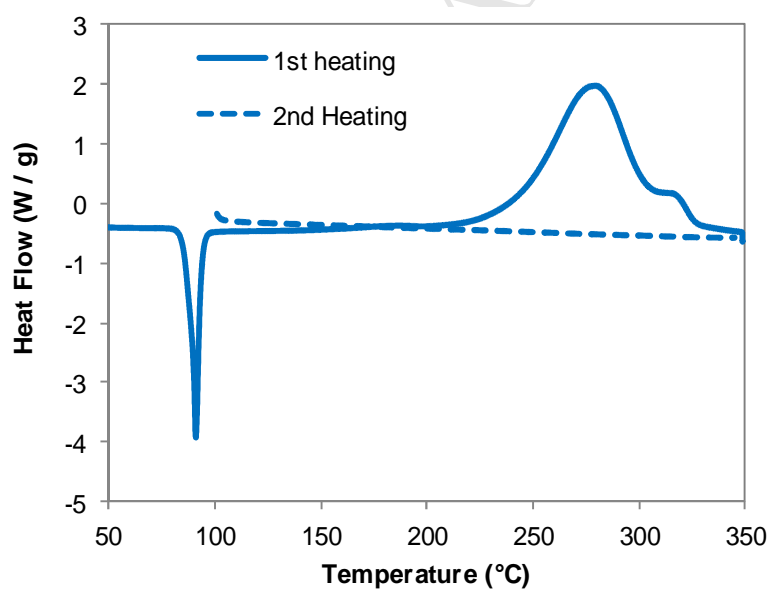
Figure 3. DSC trace of monomer **9**.
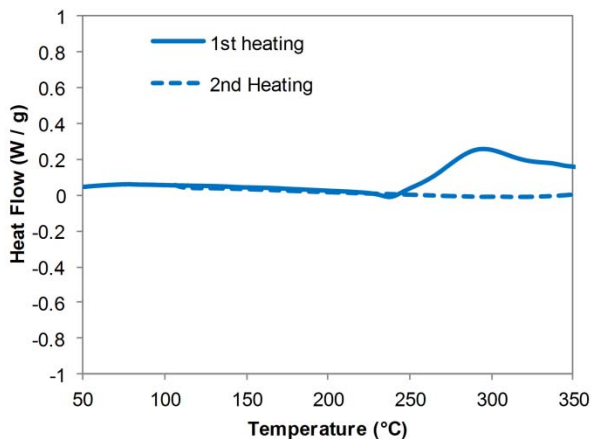
Figure 4. DSC of **9**, after curing at 210 °C for 24 hours.
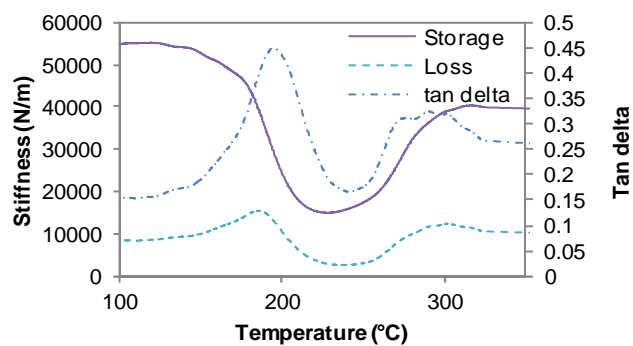
Figure 5. TMA of cured **9** after exposure to 85 °C water for 96 hours.
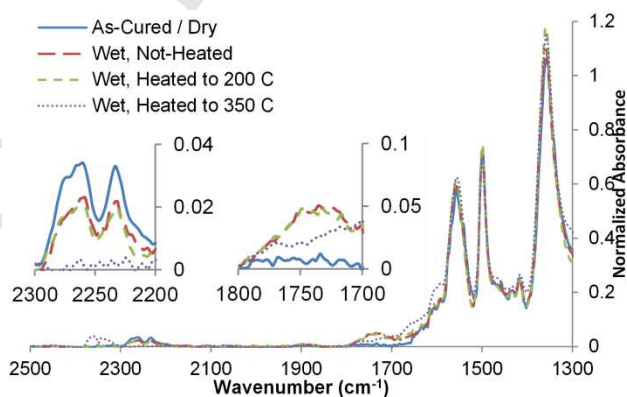
Figure 6. FT-IR scans of cured **9** at various points before, during, and after exposure to 85 °C

water and subsequent heating.
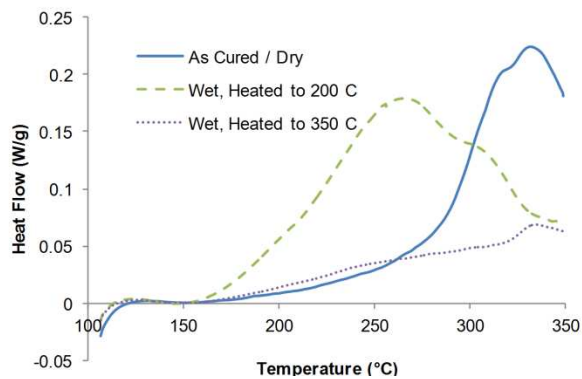
Figure 7. DSC scans (1st heating) of cured **9** at various points before, during, and after exposure to 85 °C water and subsequent heating, with the baseline (based on a 2nd heating scan) subtracted.
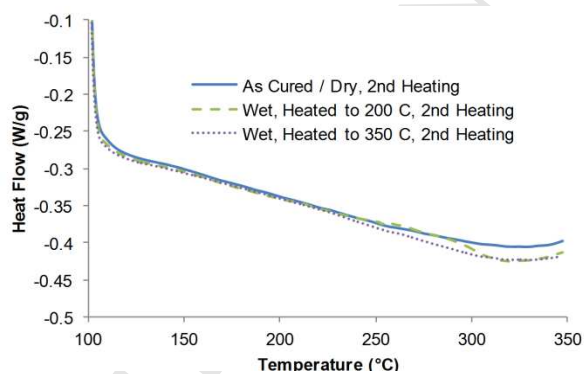
Figure 8. DSC scans (2nd heating) of cured **9** at various points before, during, and after exposure to 85 °C water and subsequent heating. The curves have been offset to coincide at low temperatures, in order to make the broad glass transitions more apparent.
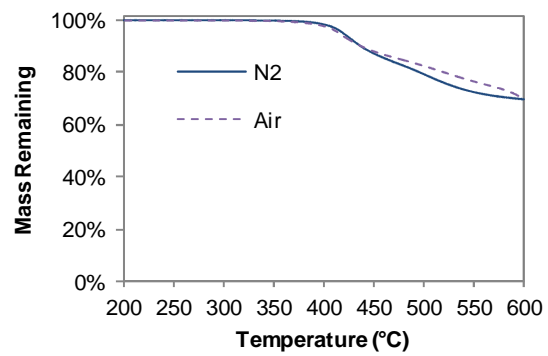
Figure 10. TGA traces of polycyanurate **9**.

Electronic Supplementary Data

Polycyanurate Networks from Dehydroanethole Cyclotrimers:

Synthesis and Characterization

Matthew C. Davis,[a] Andrew J. Guenthner,[b] Christopher M. Sahagun,[c] Kevin R. Lamison,[d] Josiah T. Reams,[d] and Joseph M. Mabry[b]

[a]*Chemistry & Materials Division, Michelson Laboratory, Naval Air Warfare Center, China Lake, California, 93555, USA.*

[b]*Air Force Research Laboratory, Aerospace Systems Directorate Edwards AFB, California, 93524, USA*

[c]*National Research Council / Air Force Research Laboratory, Aerospace Systems Directorate, Edwards AFB, California, 93524, USA*

[d]*ERC Incorporated, Edwards AFB, California, 93524,USA*

Supplementary Material Available:

Table of Contents

Experimentals Details of the Synthesis of Tricyanate 5

*1-(4-Methoxyphenyl)propyne (**2**)*

A round-bottomed flask (250 mL) equipped with magnetic stirring bar was charged with **1** (14.8 g, 100 mmol) and THF (100 mL) was cooled in an ice bath. An addition funnel was equipped and charged with Br_2 (19.2 g, 6.19 mL, 0.12 mol, 1.2 equiv) which was added dropwise over 20 min. The resulting light orange colored solution was charged into a clean addition funnel and added to an ice cold solution of KO*t*Bu (33.6 g, 3 equiv) in THF (200 mL). The cooling bath was removed and after the mixture reached rt, a heating mantle was equipped and the mixture was refluxed for 20 min. The mixture was cooled to rt and partitioned between H_2O and Et_2O. The organic layer was washed with H_2O, saturated $NaHCO_3$ and finally brine. After drying over anhydrous $MgSO_4$ the solvent was rotary evaporated leaving an orange oil. Reduced pressure distillation (0.1 torr) gave compound **2** (13.3 g) as a colorless oil. Yield: 92%. ^{1}H NMR (300 MHz, $CDCl_3$, δ, ppm): 7.32 (d, J = 9.0 Hz, 2H), 6.81 (d, J = 8.7 Hz, 2H), 3.79 (s, 3H), 2.02 (s, 3H). ^{13}C NMR (75 MHz, $CDCl_3$, δ, ppm): 159.22, 132.98, 127.06, 114.02, 84.25, 79.64, 55.37, 4.41. Anal. calcd for $C_{10}H_{10}O$: C, 82.16; H, 6.89. Found: C, 82.06; H, 7.05.

3
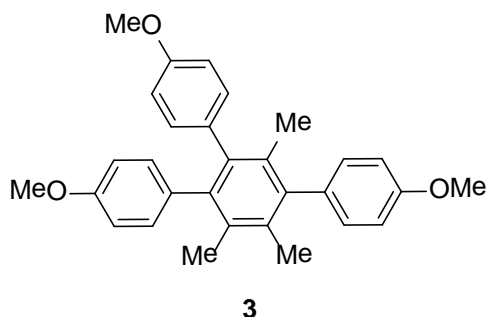
1,2,4-Tris(4-methoxyphenyl)-3,5,6-trimethylbenzene (3)

A mixture of **2** (27.28 g, 187 mmol), chlorotrimethylsilane (27 mL, 23.1 g, 212 mmol), 5% Pd/C (2 g) and 1,4-dioxane (300 mL) was protected by N_2 bubbler and refluxed overnight. The mixture was cooled to rt and filtered through diatomaceous earth. The filtrate was partitioned between H_2O and Et_2O. The organic phase was further washed with H_2O followed by saturated aqueous $NaHCO_3$ and finally brine. After charcoal treatment, the organic phase was dried over anhydrous $MgSO_4$ and rotary evaporated leaving a tan solid (23.1 g, 85%). Analysis by ^{1}H NMR of the crude showed it was composed of a mixture of compound **3** and its symmetrical isomer in a ~3:1 ratio. The crude product was dissolved in cyclohexane with some heat to form a solution which upon cooling deposited crystals of compound **3**. Compound **3** was further purified by recrystallization from cyclohexane (6.5 g). Yield: 23%. Mp: 166-168 °C. ^{1}H NMR (300 MHz, CDCl$_3$, δ, ppm): 7.16 (d, J = 8.7 Hz, 2H), 6.98 (d, J = 8.7 Hz, 2H), 6.90 (d, J = 8.7 Hz, 2H), 6.87 (d, J = 8.7 Hz, 2H), 6.69 (d, J = 8.6 Hz, 2H), 6.66 (d, J = 8.6 Hz, 2H), 3.87 (s, 3H), 3.75 (s, 3H), 3.73 (s, 3H), 2.04 (s, 6H), 1.73 (s, 3H). ^{13}C NMR (75 MHz, CDCl$_3$, δ, ppm): 158.39, 157.64, 157.58, 141.17, 140.76, 139.39, 135.05, 134.49, 134.46, 132.49, 132.44, 131.50, 131.47, 130.66, 114.02, 113.07, 113.04, 55.46, 55.28, 55.25, 19.81, 18.58, 18.40. Anal. calcd for $C_{30}H_{30}O_3$: C, 82.16; H, 6.89. Found: C, 81.86; H, 6.81.
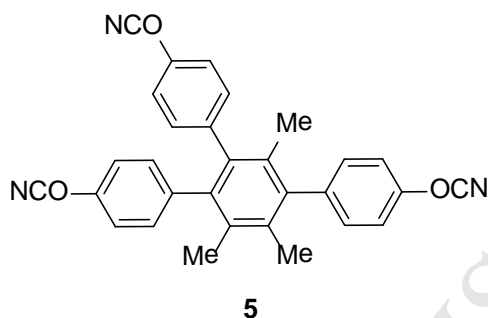
4
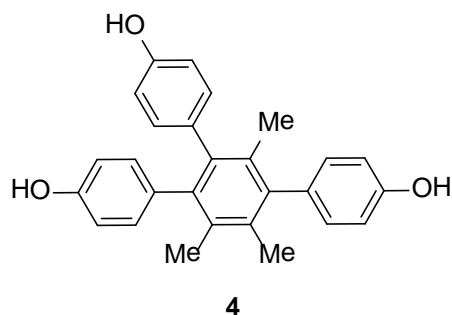
*1,2,4-Tris(4-hydroxyphenyl)-3,5,6-trimethylbenzene (**4**)*

A round-bottomed flask (250 mL) equipped with magnetic stirring bar was charged with pyridine (14.7 g, 186 mmol, 12 equiv) and H_2O (3.35 mL, 186 mmol, 12 equiv). An addition funnel was equipped which was charged with $POCl_3$ (5.7 mL, 62 mmol, 4 equiv). The addition was made over 30 min. After the mixture had cooled to rt, **3** (6.8 g, 15.5 mmol) was added in one portion. A heating mantle and condenser were equipped and the mixture was refluxed for 4 h after which time it was complete by TLC and ^{1}H NMR (aliquot in DMSO). The mixture was cooled to rt and diluted with H_2O (100 mL) which caused precipitation of a white solid. The mixture was extracted with EtOAc which dissolved the solids. The organic layer was further washed with 5% aqueous HCl followed by brine. The organic layer was dried over anhydrous $MgSO_4$ and rotary evaporated to a white solid. Residual solvent was removed by vacuum oven (60 °C, 0.1 torr) which gave compound **4** as a white powder (6 g). A suitable solvent for recrystallization was not found. Yield: 97%. ^{1}H NMR (300 MHz, CDCl$_3$/DMSO-d_6, δ, ppm): 8.82 (bs, OH), 8.55 (bs, 2OH), 7.01 (d, J = 8.4 Hz, 2H), 6.89 (d, J = 8.7 Hz, 2H), 6.77 (d, J = 8.4 Hz, 2H), 6.74 (d, J = 8.6 Hz, 2H), 6.59 (d, J = 8.1 Hz, 2H), 6.57 (d, J = 8.1 Hz, 2H), 2.03 (s, 6H), 1.71 (s, 3H). ^{13}C NMR (75 MHz, CDCl$_3$/DMSO-d_6, δ, ppm): 155.27, 154.29, 154.22, 140.49, 140.16, 138.89, 133.36, 132.87, 132.66, 132.59, 131.49, 131.47, 130.72, 130.68, 129.78, 114.88,

114.14, 114.11, 19.09, 17.81, 17.67. Anal. calcd for $C_{27}H_{24}O_3 \cdot 0.75\ H_2O$: C, 79.1; H, 6.27.

Found: C, 79.04; H, 6.55

5

*1,2,4-Tris(4-cyanatophenyl)-3,5,6-trimethylbenzene (5)*

A round-bottomed flask equipped with magnetic stirring bar was charged with **4**, acetone and

BrCN. The mixture was cooled in a bath before TEA was added dropwise over 30 min. Copious

solids precipitated (TEA·HBr). After 1 h, the mixture was partitioned between Et_2O and H_2O.

The organic layer was washed again with H_2O followed by saturated aqueous Na_2CO_3. The

organic phase was dried over anhydrous $MgSO_4$ and rotary evaporation left a colorless residue.

Recrystallization from *i*-PrOH gave compound **5** as a white microcrystalline powder. Yield:

70%. Mp: 165 °C. ^{1}H NMR (300 MHz, $CDCl_3$, δ, ppm): 7.44 (d, J = 9.0 Hz, 2H), 7.32 (d, J =

9.0 Hz, 2H), 7.18-7.00 (m, 8H), 2.02 (s, 3H), 2.01 (s, 3H), 1.65 (s, 3H). ^{13}C NMR (75 MHz,

$CDCl_3$, δ, ppm): 155.20, 151.37, 151.35, 141.03, 140.43, 140.29, 139.43, 137.61, 135.19, 132.79,

132.21, 132.16, 131.64, 131.48, 115.92, 115.04, 115.01, 109.00, 108.82, 108.80, 19.55, 18.49,

18.25. Anal. calcd for $C_{30}H_{21}N_3O_3 \cdot 0.25$ *i*-PrOH: C, 75.91; H, 4.76; N, 8.64. Found: C, 75.80;

H, 4.62; N, 8.77.

**Experimentals Details of the Synthesis of Tricyanate 9**

6
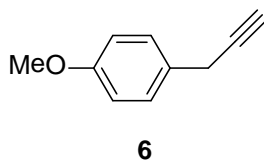
3-(4-Methoxyphenyl)propyne (6)

A round-bottomed flask (500 mL) containing Et_2O (160 mL) and **2** (20 g, 136 mmol) was cooled in a dry ice/acetone bath and 2.5 M butyllithium in hexanes solution (130 mL) was added dropwise. The color became yellow and then orange and then a precipitate formed. The cooling bath was removed and the mixture was stirred at rt for 48 h. The mixture was cooled in an ice bath and slowly quenched (2.5 h) by dropwise addition of ice cold H_2O (100 mL). Afterwards, the organic layer was separated and washed with H_2O followed by brine. After drying over anhydrous $MgSO_4$ and rotary evaporation, the remaining oil was distilled at reduced pressure (10 torr) to obtain compound **6** (18.4 g) as a colorless oil. Yield: 92%. ^{1}H NMR (300 MHz, $CDCl_3$, δ, ppm): 7.26 (d, $J = 8.8$ Hz, 2H), 6.86 (d, $J = 8.8$ Hz, 2H), 3.79 (s, 3H), 3.55 (d, $J = 2.7$ Hz, 2H), 2.17 (t, $J = 2.7$ Hz, 1H). ^{13}C NMR (75 MHz, $CDCl_3$, δ, ppm): 158.67, 133.00, 129.03, 114.21, 82.65, 70.35, 55.49, 24.13. Anal. calcd for $C_{10}H_{10}O$: C, 82.16; H, 6.89. Found: C, 82.01; H, 6.95.


7
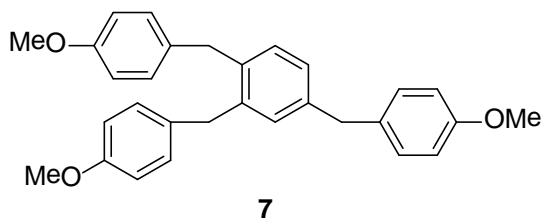
1,2,4-Tris(4-methoxybenzyl)benzene (7)

A round-bottomed flask (250 mL) equipped with magnetic stirring bar was charged with MeCN (100 mL) and CoI_2 (1 g, 10 mol%). After all the solids dissolved, $ZnBr_2$ (1.5 g, 20 mol%) was added and allowed to dissolve completely before **6** (10.19 g, 69.8 mmol) was added. Lastly, Zn dust (450 mg, 20 mol%) was added. The mixture was heated with a water bath of 60 °C. After heating for 2 h, the reaction was complete by TLC. The mixture was diluted with H_2O (500 mL) and extracted with Et_2O. The extracts were combined and dried over anhydrous $MgSO_4$ and treated with decolorizing charcoal. Rotary evaporation left a brownish oil. The product residue was chromatographed on silica gel (hexanes/EtOAc : 9/1). Rotary evaporation of the product fraction left an oil that slowly solidified to a white solid. Recrystallization from heptane gave compound **7** (5.68 g) as colorless needles. Yield: 55%. Mp 67-69 °C. ^{1}H NMR (300 MHz, $CDCl_3$, δ, ppm): 7.17-7.04 (m, 3H), 7.03-6.92 (m, 6H), 6.86-6.75 (m, 6H), 3.87 (s, 2H), 3.85 (s, 2H), 3.82 (s, 2H), 3.79 (s, 6H), 3.78 (s, 3H). ^{13}C NMR (75 MHz, $CDCl_3$, δ, ppm): 158.13, 158.06, 158.05, 139.85, 139.43, 137.31, 133.63, 132.95, 132.88, 131.26, 130.73, 130.04, 129.90, 129.79, 128.68, 127.09, 114.05, 114.00, 55.46, 40.84, 38.38, 37.89. Anal. calcd for $C_{30}H_{30}O_3$: C, 82.16; H, 6.89. Found: C, 82.30; H, 6.87.

8
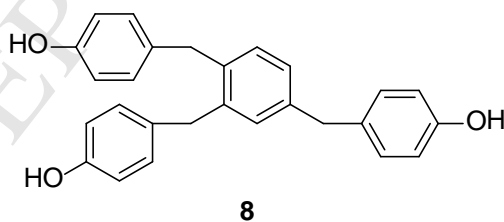
*1,2,4-Tris(4-hydroxybenzyl)benzene (**8**)*

A round-bottomed flask (250 mL) equipped with magnetic stirring bar and reflux condenser was charged with **7** (2.2 g, 5 mmol) and pyridine hydrochloride (6.9 g, 60 mmol, 12 equiv). The mixture was refluxed for 3 h, after which time the reaction was complete by TLC. The reaction

mixture was allowed to cool to ~90 °C, and then diluted with H_2O whereupon a white solid precipitated. Compound **8** (1.92 g) was collected on a filter and dried to constant weight in a vacuum oven. A suitable solvent for recrystallization could not be found. Yield: 96%. Mp 150-152 °C. ^{1}H NMR (300 MHz, DMSO-d_6, δ, ppm): 9.17 (s, OH), 9.16 (s, 2 OH), 7.05-6.9 (m, 5H), 6.9-6.8 (m, 4H), 6.7-6.6 (m, 6H), 3.8 (s, 2H), 3.7 (s, 2H). ^{13}C NMR (75 MHz, DMSO-d_6, δ, ppm): 155.44, 155.39, 139.60, 139.20, 136.96, 131.47, 130.65, 130.57, 130.43, 130.04, 129.49, 129.45, 128.15, 128.07, 126.37, 115.12, 114.96, 39.04, 37.34, 36.83. Anal. calcd for $C_{27}H_{24}O_3$: C, 81.79; H, 6.10. Found: C, 81.50; H, 5.99.

9
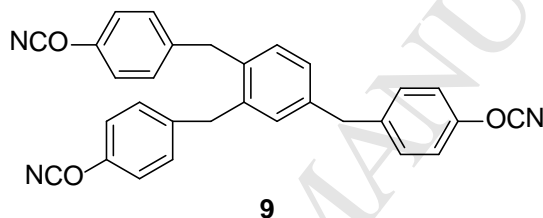
*1,2,4-Tris(4-cyanatobenzyl)benzene (**9**)*

A round-bottomed flask (1 L) equipped with magnetic stirring bar, addition funnel and N_2 bubbler was charge with **8** (9.2 g, 21 mmol), acetone (500 mL) and cooled to -78 °C bath and then BrCN (9.75 g, 92 mmol, 4 equiv) was added. Next, TEA (7.4 g, 73 mmol, 3.2 equiv) was added dropwise over 20 min. The cooling bath was removed and copious solids eventually precipitated (TEA·HBr salt). After allowing to warm to rt, the mixture was poured into a separatory funnel and diluted with Et_2O (500 mL) and H_2O (500 mL). The organic layer was washed again with H_2O (500 mL) and then brine (500 mL). The organic layer was dried over anhydrous $MgSO_4$ and rotary evaporated. To the remaining colorless oil in the flask was added Et_2O (100 mL) and after agitation the product precipitated. The white solid (3.8 g) was collected on a medium porosity glass frit. Recrystallization from isopropanol/MeCN (15/1) gave

compound **9** as microcrystalline needles. Yield: 35%. Mp 85-87 °C. ^{1}H NMR (300 MHz, CDCl$_3$, δ, ppm): 7.29-7.16 (m, 8H), 7.13-7.03 (m, 6H), 6.93 (s, 1H), 3.98 (s, 2H), 3.89 (s, 2H), 3.88 (s, 2H). ^{13}C NMR (75 MHz, CDCl$_3$, δ, ppm): 151.55, 151.49, 140.06, 139.42, 139.29, 129.23, 138.42, 136.43, 131.47, 131.32, 130.91, 130.61, 130.52, 127.87, 115.56, 115.54, 115.52, 109.06, 109.01, 40.75, 38.40, 37.99. Anal. calcd for C$_{30}$H$_{21}$N$_3$O$_3$: C, 76.42; H, 4.49; N, 8.91. Found: C, 76.05; H, 4.40; N, 9.03.
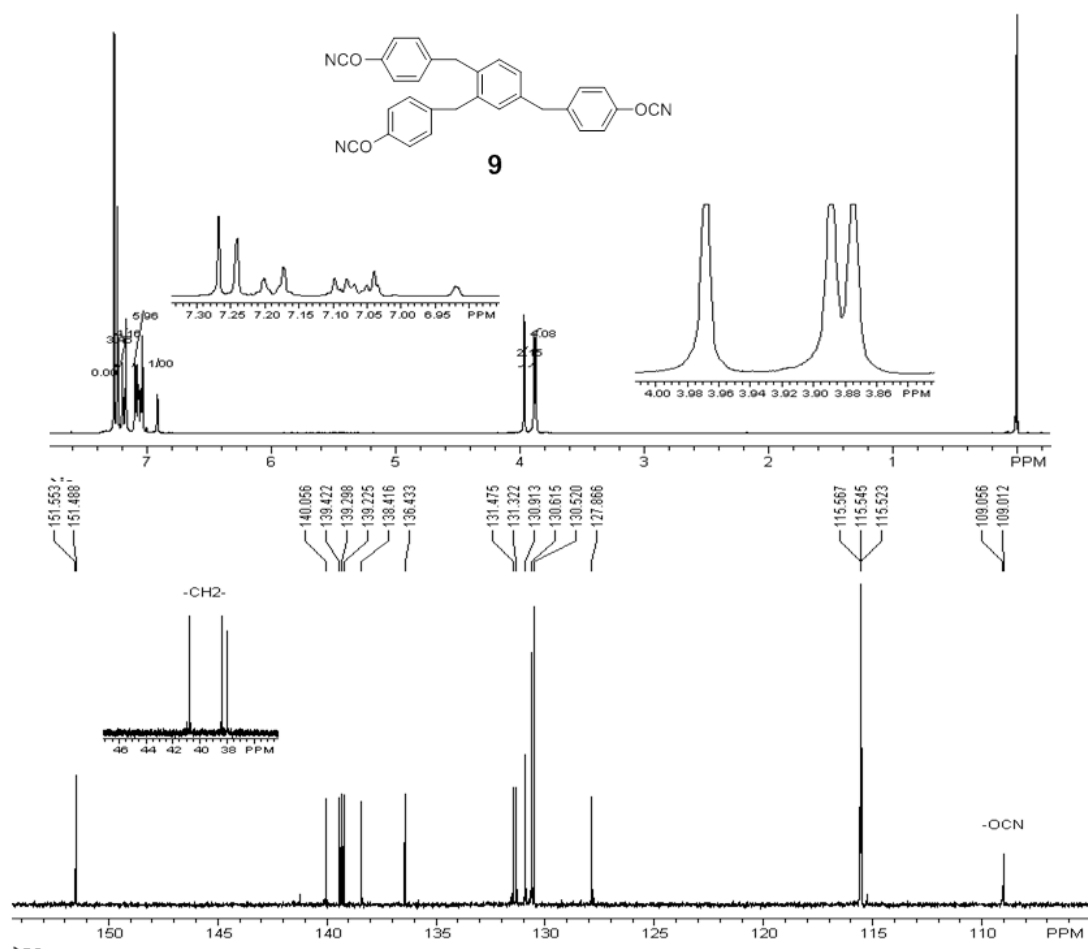
Figure S1. ^{1}H and ^{13}C NMR of tricyanate **9**.
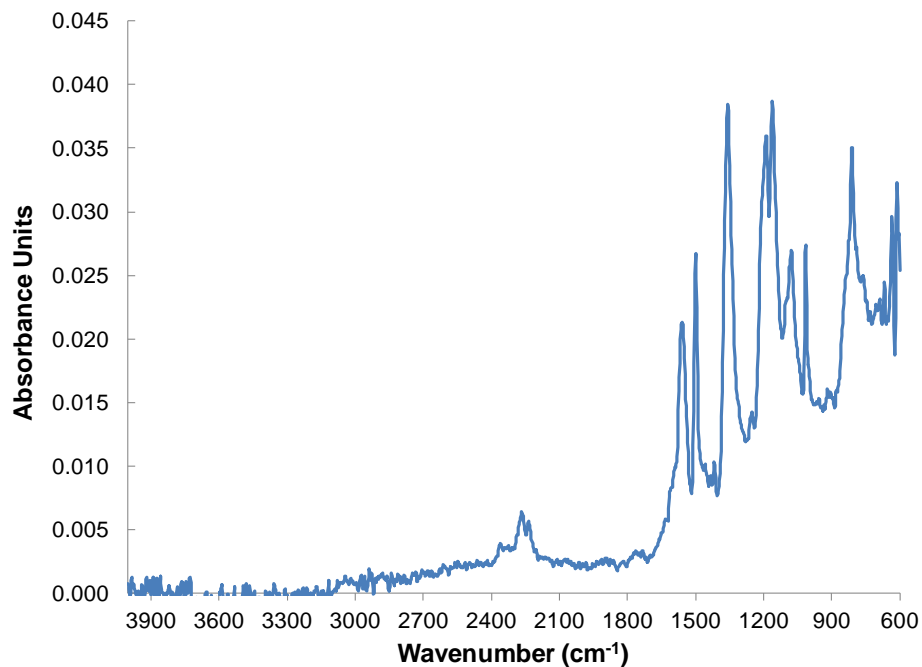
Figure S2. FT-IR spectrum of cured **9**.
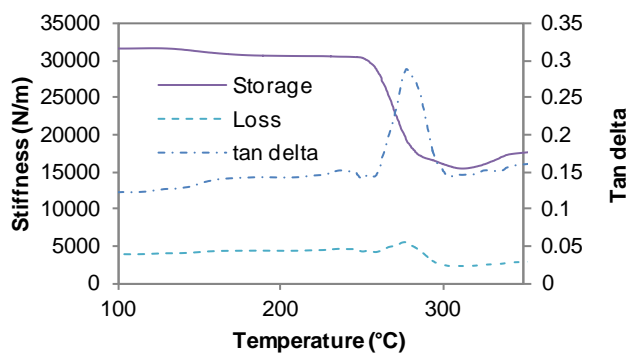
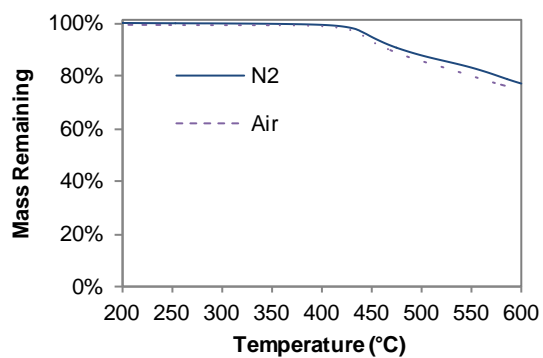Figure S3**.** TMA of 'as cured' monomer **9**

Figure S4. TGA trace of cured **10**.

Determination of diBenedetto equation parameters

Samples (~5 mg) of uncured **9** were heated as quickly as possible to a given cure temperature, then held isothermally for 30 minutes and cooled as quickly as possible. The same sample was then heated to 350 °C at 10 °C / min, cooled to 100 °C at 10 °C / min, then re-heated to 350 °C at 10 °C / min. The re-heating scan, offset by a pre-determined value, was used as a baseline. The difference between the heat evolved during the first heating ramp to 350 °C and the baseline was then used for integration of the residual heat of cure. The pre-determined value for the offset was chosen based on the smallest correction that ensured no negative values in the integration, and at least one zero value (which was then chosen as the starting point for the integration), with the maximum temperature in the second scan as the ending point. A detailed explanation and illustration of this baseline and integration procedure is given elsewhere [see the Supporting Information of Guenthner AJ, Davis MC, Ford MD, Reams JT, Groshens TJ, Baldwin LC, et al. Macromolecules 2012;45:9707-18].

During the initial heating to 350 °C, the glass transition temperature of the partially cured sample was either apparent as a step change in heat capacity, or, when no step change was apparent, was equated with the onset temperature of residual cure. For determination of the diBenedetto equation, cure temperatures of 210 °C, 220 °C, 230 °C, 240 °C, 250 °C, and 260 °C were used. The diBenedetto equation is:

$$\frac{(T_g - T_{g0})}{(T_{g\infty} - T_{g0})} = \frac{\lambda \alpha}{1 - (1-\lambda)\alpha}$$

where T_{g0} and $T_{g\infty}$ represent the glass transition temperatures of the monomer and fully cured network, respectively, and in which λ is effectively an adjustable parameter ($0 \leq \lambda \leq 1$). The value of $T_{g\infty}$ was fixed at 362 °C based on data from thermomechanical analysis of a fully cured

sample. The values of T_{g0} and λ were determined by minimization of squared residuals using a brute force search with increments of 0.01 for λ and 10 °C for T_{g0}. The uncertainties were determined by noting the change (independently) in each parameter that led to an increase of 1 in the square of the characteristic deviation (that is, the deviation divided by a characteristic measurement uncertainty, 10 °C in this case). The reasonableness of this procedure was checked by evaluating the theoretical curve at the upper and lower bounds of uncertainty for each parameter and noting that at these bounds, the fit to the data was at the limit of plausibility according to a simple visual inspection.

The resulting best fit plot of glass transition temperature as a function of conversion is shown in Figure S5. The diBenedetto parameter values $T_{g0} = 10 \pm 10$ °C and $\lambda = 0.44 \pm 0.06$.
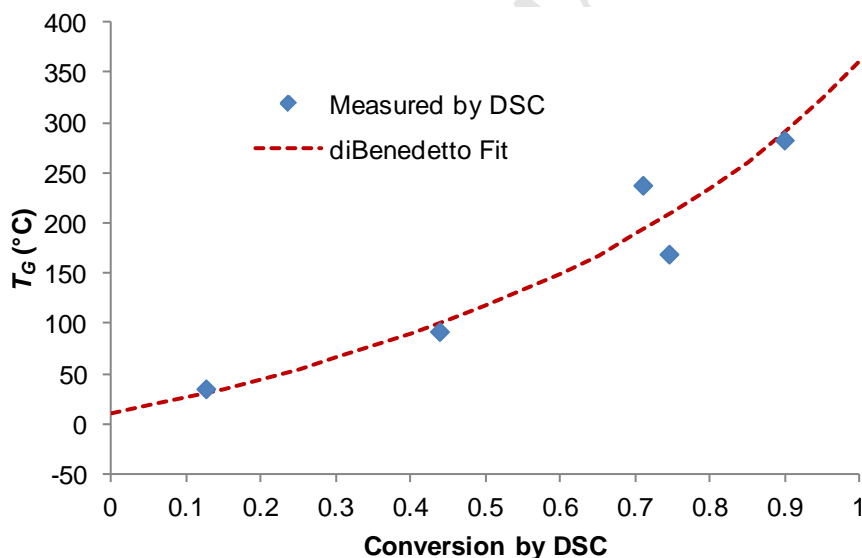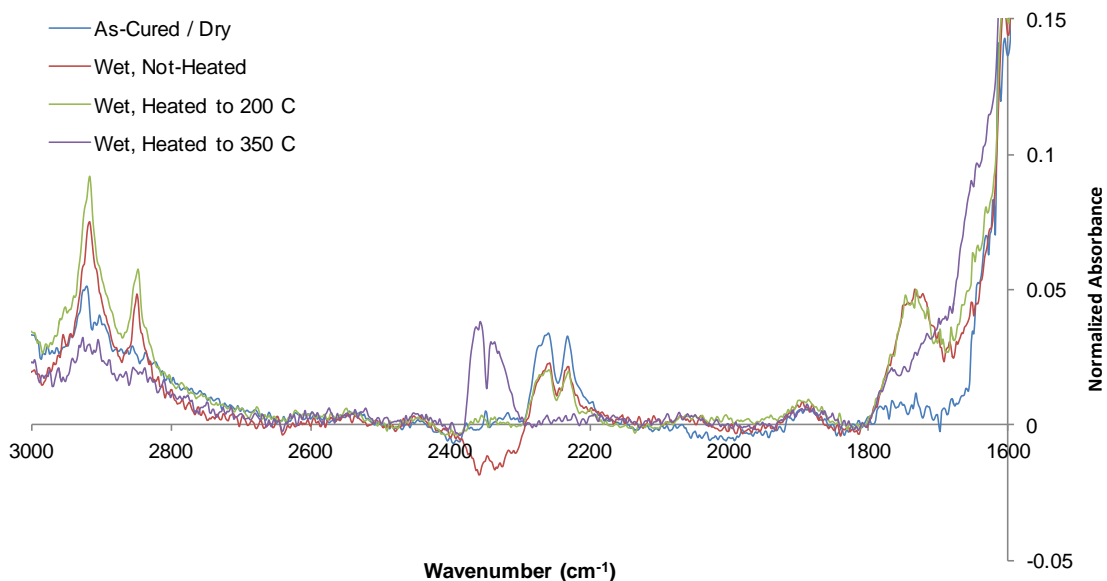

Figure S5. diBenedetto equation plot for **9**.

Figure S6. FT-IR spectra of cured **9** before and after hygrothermal exposure and subsequent heating, zoomed in on the 1600 cm^{-1} – 3000 cm^{-1} region. The peaks at 2300 cm^{-1} – 2400 cm^{-1} are due to CO_2.
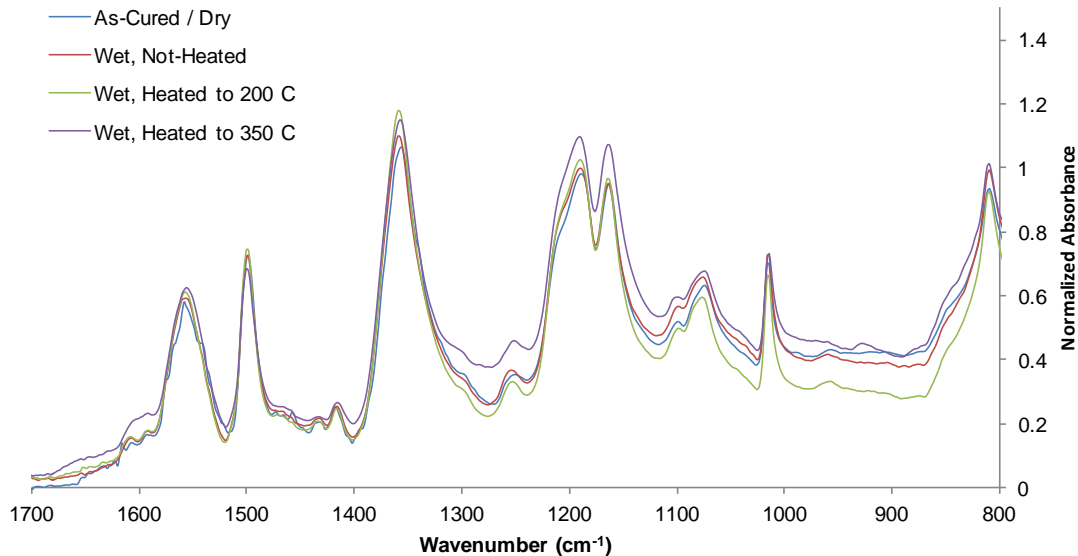

Figure S7. FT-IR spectra of cured **9** before and after hygrothermal exposure and subsequent heating, zoomed in on the 800 cm^{-1} – 1700 cm^{-1} region.
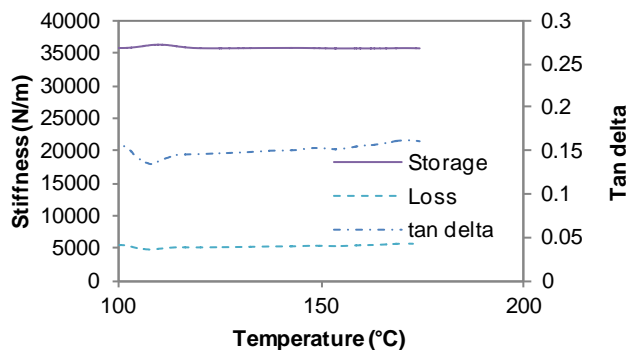
Figure S8. TMA trace of **9** cured to 87% conversion, then immersed in 85 °C water for 96 hours (first heating to 200 °C, after which a portion of the sample was removed for analysis). Due to thermal lag, the average sample temperature does not reach 200 °C even when the set-point reaches 200 °C and the run terminates).
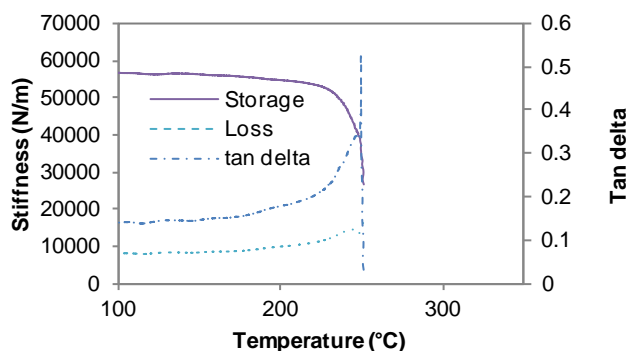

Figure S9. TMA trace of **9** cured to 87% conversion, then immersed in 85 °C water for 96 hours, then heated to 200 °C (re-heating to 350 °C, after which a portion of the sample was removed for analysis). Note that the TMA probe becomes disengaged at about 260 °C due to a sudden release of water vapor.
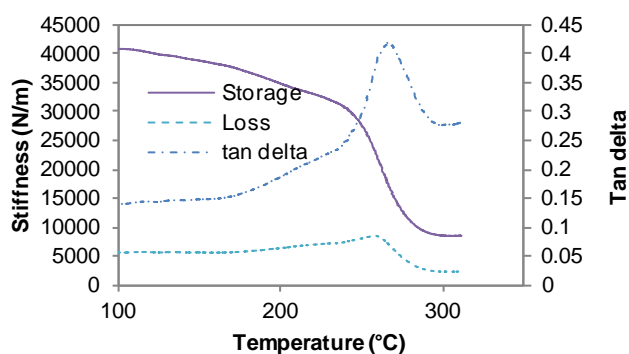

Figure S10. TMA trace of **9** cured to 87% conversion, then immersed in 85 °C water for 96 hours, then heated to 200 °C and re-heated to 350 °C (final scan to assess T_g).